



# Donnan Dialysis for scaling mitigation during electrochemical ammonium recovery from complex wastewater

Mariana Rodrigues<sup>a,b</sup>, Aishwarya Paradkar<sup>a</sup>, Tom Sleutels<sup>a</sup>, Annemiek ter Heijne<sup>b</sup>, Cees J. N. Buisman<sup>a,b</sup>, Hubertus V.M. Hamelers<sup>a,b</sup>, Philipp Kuntke<sup>a,b,\*</sup>

<sup>a</sup> Wetsus, European Centre of Excellence for Sustainable Water Technology, Oostergoweg 9 8911MA Leeuwarden P.O. Box 1113, 8900 CC Leeuwarden, the Netherlands

<sup>b</sup> Environmental Technology, Wageningen University, Bornse Weilanden 9 6708 WG Wageningen P.O. Box 17, 6700 AA Wageningen, the Netherlands

## ARTICLE INFO

### Keywords:

Inorganic scaling  
Ammonium recovery  
Extended operation  
Donnan dialysis

## ABSTRACT

Inorganic scaling is often an obstacle for implementing electrodialysis systems in general and for nutrient recovery from wastewater specifically. In this work, Donnan dialysis was explored, to prevent scaling and to prolong operation of an electrochemical system for TAN (total ammonia nitrogen) recovery. An electrochemical system was operated with and without an additional Donnan dialysis cell, while being supplied with synthetic influent and real digested black water. For the same Load Ratio (nitrogen load vs applied current) while treating digested black water, the system operated for a period three times longer when combined with a Donnan cell. Furthermore, the amount of nitrogen recovered was higher. System performance was evaluated in terms of both TAN recovery and energy efficiency, at different Load Ratios. At a Load Ratio 1.3 and current density of 10 A m<sup>-2</sup>, a TAN recovery of 83% was achieved while consuming 9.7 kWh kg<sup>-1</sup>.

## 1. Introduction

Towards closing the resources cycle for a circular economy, our considered “waste” water has become a source of nutrients and energy. (Cordell et al., 2011; Galloway et al., 2008; Gao et al., 2019; Maurer et al., 2003; Moges et al., 2018; Theregowda et al., 2019) Amongst all the nutrients present in wastewater, phosphorus and nitrogen are of the utmost importance as they play a vital role in plant growth. As phosphorus is a scarce nutrient, considerable efforts were taken in the last two decades to recover it from our wastewater. (Cordell et al., 2009; Egle et al., 2016; Wilfert et al., 2015) Nitrogen (N<sub>2</sub>), however, amounts to 78% of all gasses present in the atmosphere and it can be artificially fixed by the Haber-Bosch process into reactive nitrogen forms (e.g. NH<sub>3</sub> and NH<sub>4</sub><sup>+</sup>) to be used as fertilizer. (Cordell et al., 2009; Kuntke et al., 2018) In order to decrease its environmental effect, such as eutrophication, nitrogen has been removed from wastewater via nitrification-denitrification or Anammox at wastewater treatment plants (WWTP). (Ahn, 2006; Giddey et al., 2013; Rodríguez Arredondo et al., 2017, 2015) These aforementioned nitrogen removal processes are energy intensive and contribute N<sub>2</sub>O emissions to the atmosphere. In addition, up to 2% of the energy produced worldwide is consumed by the Haber-Bosch process. (Kuntke et al., 2017; Kuntke et al., 2018;

Shipman and Symes, 2017)

Source separation of wastewater has been investigated as a promising concept to allow for energy efficient wastewater treatment and nutrient recovery. (Larsen et al., 2015; Zeeman and Kujawa-Roeleveld, 2011) Phosphorus and nitrogen were recovered from source separated streams such as black water (combined feces and urine) or urine (Kuntke et al., 2018; Ledezma et al., 2015; Tarpeh et al., 2018). Black water is responsible for up to 70% of chemical oxygen demand (COD), 80% phosphorous and 90% nitrogen found in conventional wastewater (de Graaff et al., 2010; Vlaeminck et al., 2009).

Phosphate recovery was successfully described by forming struvite (Zamora et al., 2017) or calcium phosphate granules (Cunha et al., 2019; Lei et al., 2019). Nonetheless, after phosphate recovery in these processes, almost all the ammonium remains in solution (Cunha et al., 2019; Moges et al., 2018). An electrochemical system (ES) has been proposed to recover the remaining ammonia and ammonium (total ammonia nitrogen, TAN), as it does not require chemical dosing and requires less energy than NH<sub>3</sub> stripping, chemical precipitation or adsorption (Kuntke et al., 2018; Lei et al., 2007; Rodríguez Arredondo et al., 2015; Wasielewski et al., 2016). However, digested black water or urine, although rich in nitrogen, also contain other several ions (incl. Ca<sup>2+</sup>, Mg<sup>2+</sup>, K<sup>+</sup>, Na<sup>+</sup>, CO<sub>3</sub><sup>2-</sup>, Cl<sup>-</sup>, SO<sub>4</sub><sup>2-</sup>, PO<sub>4</sub><sup>3-</sup>) (Casademont et al., 2008; Choi et al., 2011;

\* Corresponding author.

E-mail address: [philipp.kuntke@wur.nl](mailto:philipp.kuntke@wur.nl) (P. Kuntke).

<https://doi.org/10.1016/j.watres.2021.117260>

Received 20 February 2021; Received in revised form 25 April 2021; Accepted 12 May 2021

Available online 17 May 2021

0043-1354/© 2021 The Author(s). Published by Elsevier Ltd. This is an open access article under the CC BY license (<http://creativecommons.org/licenses/by/4.0/>).

Luther et al., 2015; Rodríguez Arredondo et al., 2017). The presence of bivalent ions was previously reported to interfere with electrodialysis process and therefore nutrient recovery, as calcium and magnesium ions are more susceptible to the electric field and CEMs are more selective for divalent ions (Ping et al., 2013; Rijnaarts et al., 2018; Yang et al., 2014). While some studies consider the concentration of calcium and magnesium negligible due to upstream precipitation such as struvite (Tarpeh et al., 2018; Thompson Brewster et al., 2017), it has been shown that under alkaline conditions low concentrations ( $0.02 \text{ M Ca}^{2+}$ ) are sufficient to scale ion exchange membranes (Andreeva et al., 2017; Luther et al., 2015; Pan et al., 2020; Shaposhnik et al., 2002). Moreover, the presence of  $\text{Mg}^{2+}$  facilitates the formation of calcium carbonate, even at very low concentrations of both ions and slightly above pH neutrality (Ayala-Bribiesca et al., 2006; Casademont et al., 2007). The cation exchange membranes (CEM) used in an ES for TAN recovery are not species selective and transport all cations, which accumulate in the concentrate/cathode solution. The alkaline pH in the concentrate results in the formation of inorganic scaling on the CEM (e.g. precipitation of insoluble salts such as calcite, gypsum, struvite etc.) (Thompson Brewster et al., 2017).

When scaling forms on the surface of ion exchange membranes, the stack electrical resistance increases, leading to an increase in energy input (Andreeva et al., 2017; Asraf-Snir et al., 2018). Some solutions were proposed to address this problem, such as filtration, coagulation and flocculation, the use of anti-scalants, and chemical cleaning of the membranes by in situ use of acidic or alkaline chemicals (Andreeva et al., 2018; Thompson Brewster et al., 2017; Tran et al., 2013). Despite having several options, all imply additional cost and/or operational interruption in order to regenerate or even replace the scaled membranes (Andreeva et al., 2018; Thompson Brewster et al., 2017). The implementation of electrochemical systems for nutrient recovery applications are thus limited as so far no satisfactory solution has been identified (Andreeva et al., 2018; Thompson Brewster et al., 2017).

During electrodialysis ammonium and other cations are transported toward the cathode and accumulate in a concentrated solution. While ammonia can be extracted through a gas permeable membrane, cations

like sodium or potassium will continuously accumulate in this concentrated solution when current is constantly supplied. Donnan dialysis (DD) has been previously described to promote the exchange of ammonium in the feed with other cations (such as  $\text{Na}^+$  and  $\text{K}^+$ ) accumulated on the concentrate side (Cox and Dinunzio, 1977; Rijnaarts et al., 2018; Rodrigues et al., 2020b). During Donnan dialysis, no current is applied and the ions move due to an electrochemical potential difference, generated by a concentration gradient formed between the feed and the concentrate during electrodialysis (Campione et al., 2018; Chen et al., 2020; Rodrigues et al., 2020b). Hence, also bivalent cations accumulated in a concentrate solution can exchange with monovalent cations from the feed solution (Rodrigues et al., 2020b). In reverse electrodialysis, Rijnaarts et al., 2019 used Donnan dialysis as a pre-treatment step to remove  $\text{SO}_4^{2-}$  from feedwater and were able to achieve 76% reduction of the bivalent ion content, limiting the occurrence of scaling (Rijnaarts et al., 2018). The purpose of this research was to assess whether Donnan dialysis can be used as pre-treatment for scaling mitigation when a complex ammonia rich influent is supplied to an ES without further energy consumption and need for chemical addition.

## 2. Materials and methods

### 2.1. Experimental setup

The TAN recovery system consisted of previously described electrodialysis (ED) cell and a transmembrane chemisorption (TMCS) module, which is presented in full detail in the supplementary information Appendix A – A.1. Experimental Setup (Kuntke et al., 2017; Rodrigues et al., 2020b). An additional cell was introduced in the system for Donnan dialysis, presented in Fig. 1.

The electrodialysis cell included a feed and a concentrated compartment (1.2 cm thickness each) and separated by a cation exchange membrane (Fumasep FKB-PK-130, FUMATECH BWT GmbH, Bietigheim-Bissingen, Germany). The anode and cathode compartment included a platinum (Pt) coated titanium mesh electrode measuring ( $9.8 \text{ cm} \times 9.8 \text{ cm}$ ,  $5 \text{ mg Pt cm}^{-2}$  Magneto Special Anodes BV, The

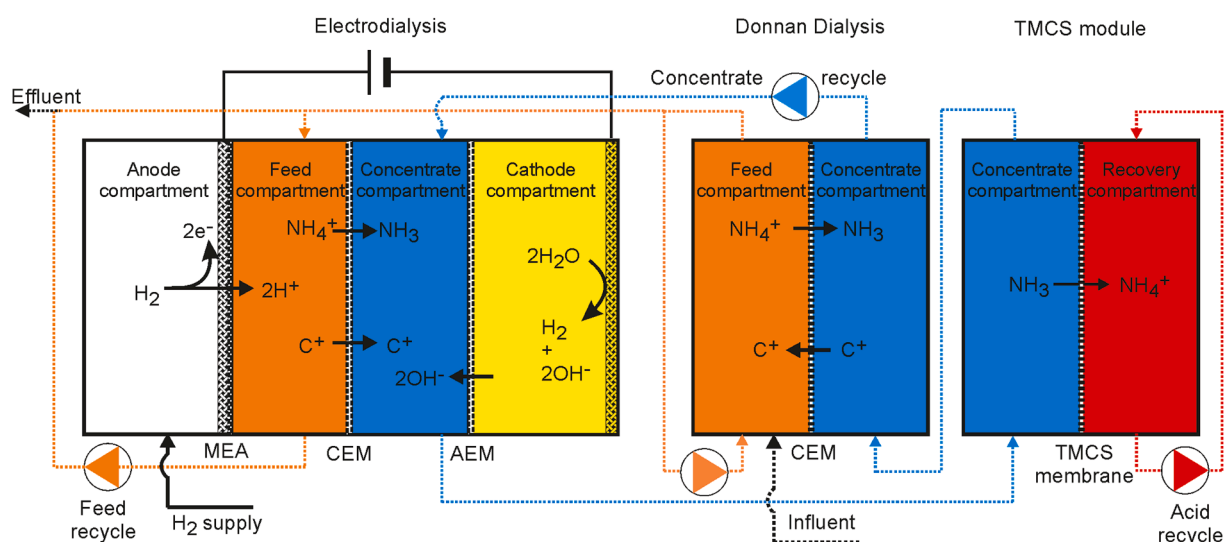


**Fig. 1.** Electrochemical system with hydrogen gas recycling for TAN recovery including Donnan dialysis (DD) cell. Oxidation of hydrogen occurs at the anode of the electrodialysis cell, where protons are generated and transferred over a membrane electrode assembly (MEA) to the feed compartment. These protons acidify the influent to form ammonium ( $\text{NH}_4^+$ ). The  $\text{NH}_4^+$  can then be transported over a cation exchange membrane (CEM) to a concentrate solution. Other cations (represented here as  $\text{C}^+$ ) are also transported as the CEM is not species selective. Simultaneously, the  $\text{OH}^-$  ions formed at the cathode, are transported via an anion exchange membrane (AEM) to the concentrate solution increasing the pH. Later, the ammonia formed in the concentrate is recovered through a Transmembrane Chemisorption (TMCS) unit, which consists of a gas permeable hydrophobic membrane. Once the ammonia is transferred over the TMCS, the concentrated solution is supplied to the DD cell. Here, the previously accumulated cations such as sodium or magnesium, return to the feed compartment due to a concentration gradient. The influent was first supplied to the feed compartment of the DD cell to achieve a higher concentration gradient and exchange the cations from the concentrate side with ammonium from the feed side. This configuration allows the hydrogen gas formed at the cathode compartment to be later recycled to the anode compartment, conserving energy.

Netherlands) in a 0.2 cm x 10 cm x 10 cm compartment. The ion exchange membranes had a projected surface area of 100 cm<sup>2</sup>. The anode was separated from feed compartment by a Membrane Electrode Assembly (MEA). The concentrate compartment was separated from cathode compartment by an anion exchange membrane (Fumasep FAB-PK-130, FUMATECH BWT GmbH, Bietigheim-Bissingen, Germany).

The DD cell consisted of feed and concentrate compartments, made of poly methyl methacrylate. Each compartment had a size of 21 cm x 21 cm x 2.5 cm and a machined flow field of 10 cm x 10 cm x 0.2 cm. Feed and concentrate compartments were separated by a 15 cm x 15 cm CEM (Fumasep FKB-PK-130, FUMATECH BWT GmbH). During DD, the influent was first supplied to the feed compartment of the DD cell.

In order to supply influent and recirculate feed, concentrate, cathode and acid solutions, four Masterflex peristaltic pumps (Masterflex L/S, Metrohm Applikon BV, Schiedam, The Netherlands) were used. The recirculation flow rate for feed, concentrate, cathode and acid was 160 mL min<sup>-1</sup>.

The influent flow is presented in Table 1, according to the used Load Ratio.

## 2.2. Experimental strategy

The system was supplied with the effluent of a lab scale Upflow Anaerobic Sludge Blanket digestion reactor (UASB reactor) (Wetsus, European center of Excellence for Sustainable Water Technology, Leeuwarden, The Netherlands) used for phosphate recovery as calcium granules as described in Cunha et al., 2018. The addition of calcium to the reactor results in the production of calcium phosphate granules, while removing 89% of the phosphate (Cunha et al., 2018). Furthermore, > 80% of the total COD is removed and around 0.5 g COD-CH<sub>4</sub> g<sup>-1</sup> COD<sub>Total</sub>-BW was produced (Cunha et al., 2019, 2018). The effluent (digested black water) consisted mainly of NH<sub>4</sub><sup>+</sup> (1 g L<sup>-1</sup>), Cl<sup>-</sup> (0.463 g L<sup>-1</sup>), Na<sup>+</sup> (0.290 g L<sup>-1</sup>), K<sup>+</sup> (0.230 g L<sup>-1</sup>), Ca<sup>2+</sup> (0.046 g L<sup>-1</sup>), Mg<sup>2+</sup> (0.024 g L<sup>-1</sup>), PO<sub>4</sub><sup>3-</sup> (0.051 g L<sup>-1</sup>), SO<sub>4</sub><sup>2-</sup> (0.038 g L<sup>-1</sup>), and COD (0.419 g L<sup>-1</sup>). Therefore, it consists of a complex ionic and organic matrix suitable to study nutrient recovery from a complex wastewater stream.

Although, solids were retained in the UASB reactor, the effluent of the UASB passed through a 10-micron filter before being supplied to the ES with (w/) and without (w/o) DD.

The system was also operated with synthetic influent (to compare the transport over the membrane). Synthetic influent mimicked the digested black water collected after the UASB reactor without bivalent cations and an organic carbon source. The synthetic black water consisted of 2.75 g L<sup>-1</sup> (NH<sub>4</sub>)<sub>2</sub>CO<sub>3</sub>, 0.08 g L<sup>-1</sup> K<sub>2</sub>SO<sub>4</sub>, 0.47 g L<sup>-1</sup> KCl, 0.31 g L<sup>-1</sup> NaCl, and 0.5 g L<sup>-1</sup> Na<sub>2</sub>CO<sub>3</sub>.

Table 1 includes all sets of experiments performed and studied for this research. The experiments were carried out at a constant current density of 10 A m<sup>-2</sup>. Choosing 10 A m<sup>-2</sup> allowed to operate the ES

**Table 1**

Experiments performed using an electrodialysis cell with or without the DD cell at different Load Ratio.

Setup	Influent	Load Ratio	Inflow (ml min <sup>-1</sup> )	HRT (h)	Volume (L day <sup>-1</sup> )
ED	Synthetic Influent	1	1.63	4.1	2.4
	Black Water	1	1.63	4.1	2.4
ED + DD	Synthetic Influent	1	1.63	4.1 (ED) 1 (DD)	2.4
	Black Water	0.5	3.97	1.7 (ED) 0.4 (DD)	4.7
		1	1.63	4.1 (ED) 1 (DD)	2.4
		1.3	1.2	5.6 (ED) 1.4 (DD)	1.7
		1.5	0.96	6.9 (ED) 1.7 (DD)	1.4

system continuously for a longer period considering the effluent flow rate (L d<sup>-1</sup>) of the UASB reactor.

## 2.3. Calculations

The calculations were based on earlier work and explained in detail in the Supporting Information, Appendix A – A.2. Calculations.

### 2.3.1. Load ratio

Load Ratio ( $L_N$ ) is the ratio of applied current density to the TAN loading. The Load Ratio determines to a large extent the performance of the ES system (removal, energy consumption, Coulombic efficiency) (Rodríguez Arredondo et al., 2017). A Load Ratio of one means the amount of current applied to the system is equal to the total charge supplied as TAN. When  $L_N < 1$  more TAN is present than the electrons supplied to the cell, conversely when  $L_N > 1$  the system is supplied with an excess of current. Load Ratio can be determined using the following formula:

$$L_N = \frac{j \times A_m}{C_{\text{TAN, influent}} \times Q_{\text{influent}} \times F}$$

Where,  $j$  is the current density (A m<sup>-2</sup>),  $C_{\text{TAN, influent}}$  is the concentration of TAN (mol L<sup>-1</sup>) in the influent,  $Q_{\text{influent}}$  is the influent flow rate (L L<sup>-1</sup>),  $F$  is the Faraday constant (C mol<sup>-1</sup>) and  $A_m$  is the surface area of CEM (m<sup>2</sup>).

## 2.4. Chemical analysis

Samples were collected daily from influent and effluent of the DD cell, effluent of the electrodialysis cell, concentrate, cathode, and acid. The samples were analyzed for cations (NH<sub>4</sub><sup>+</sup>, Na<sup>+</sup>, K<sup>+</sup>, Ca<sup>2+</sup>, Mg<sup>2+</sup>) and anions (NO<sub>3</sub><sup>-</sup>, NO<sub>2</sub><sup>-</sup>, Cl<sup>-</sup>, SO<sub>4</sub><sup>2-</sup>, PO<sub>4</sub><sup>3-</sup>) using a Metrohm Compact IC Flex 930 with a cation column (Metrosep C 4–150/4.0) and a Metrohm Compact IC 761 with an anion column (Metrosep A Supp 5–150/4.0) respectively. The samples were also analyzed for organic carbon, inorganic carbon, non-purgeable organic carbon and total carbon using a TOC analyzer (TOC-L CPH, Shimadzu BENELUX, 's-Hertogenbosch, The Netherlands). When supplying the ES with black water all samples were also analyzed for metals, using inductively coupled plasma optical emission spectrometry (ICP-OES), and for chemical oxygen demand (COD), using a cuvette test kit LCK 414 and a spectrophotometer DR3900 (HACH NEDERLAND, Tiel, The Netherlands).

## 3. Results

### 3.1. Donnan dialysis slows CEM scaling allowing longer operation

The ES was operated at a Load Ratio one at 10 A m<sup>-2</sup> with and without the DD cell using digested black water as influent. Fig. 2 shows the measured cell voltage and the potential losses in the cell including MEA overpotential ( $\eta_{\text{MEA}}$ ) and cathode overpotential ( $\eta_{\text{cathode}}$ ), ionic losses ( $E_{\text{ion}}$ ), pH losses ( $E_{\text{pH}}$ ) and the membranes potential ( $E_{\text{membrane}}$ ) of the ED cell at three distinct regions. The potential losses were calculated as explained in the Supporting Information, Appendix A – A.2. Calculations.

After 12 h the measured voltage spiked to more than 5 V and the operation was therefore interrupted, when operating the system with digested black water without a DD cell (Fig. 2). This cell voltage of 5 V can be associated with pH change in the concentrate compartment and scaling formation. When operating the system with Donnan dialysis at the same conditions, scaling was delayed by almost 30 h, meaning the period of continuous operation was extended by more than three times that without Donnan. The potential losses showed an increase of the membrane resistance ( $E_{\text{membrane}}$ ) over time, Fig. 2. By SEM EDS analysis of the CEM, it was clear that the membrane was scaled with calcium salts (SI, Appendix B -Figure A.1). Some of the calcium present in the UASB

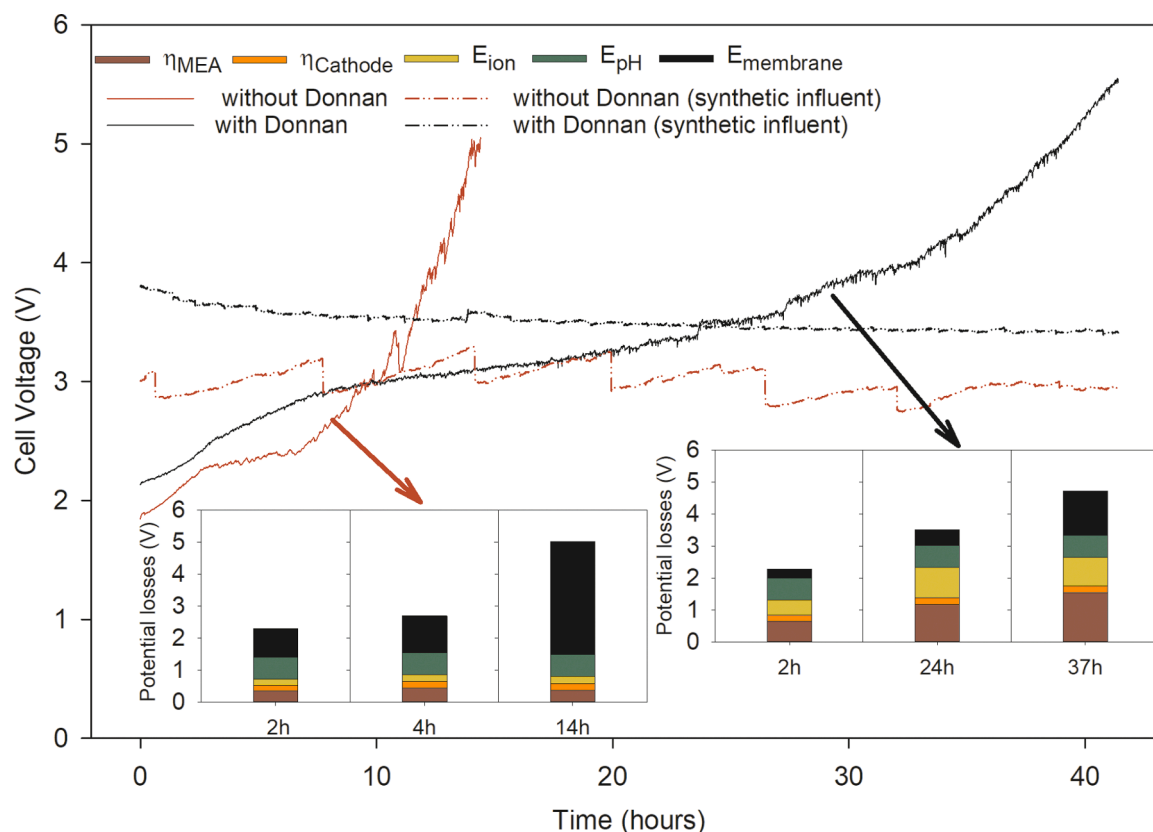


**Fig. 2.** Electrodialysis cell voltage (V) with and without Donnan dialysis over time at  $L_N=1$  and  $10 \text{ A m}^{-2}$ . The ED cell voltage is the result of electrode overpotential ( $\eta_{\text{MEA}}$  and  $\eta_{\text{cathode}}$ ), ionic losses ( $E_{\text{ion}}$ ), pH losses ( $E_{\text{pH}}$ ) and membrane potential ( $E_{\text{membrane}}$ ). The potential losses were calculated after 2, 4 and 14 h for the ES while operating without Donnan dialysis. With Donnan dialysis, the potential losses were calculated after 2, 24 and 37 h. Three regions were distinguished during the operation period: 1) an initial increase until stable state, 2) stable operation and 3) voltage ramp up as the scale blocks the CEM.

reactor effluent (influent of ES) precipitated in the form of calcium carbonate ( $\text{CaCO}_3$ ) on the CEM. While operating with synthetic influent, the ES performed at a constant voltage of approximately 3 V both with and without Donnan dialysis.

When supplied with digested black water, it was not possible to operate the ES system for more than 12 h, at the same Load Ratio and current density again due to scaling on the CEM. As the membrane scales, the effective area of the membrane where the ions can be exchanged is therefore reduced. (Ayala-Bribiesca et al., 2006) This limits the overall ion transport and in-turn affects the TAN recovery. Nevertheless, within this 12 h stable period of operation, 79% TAN recovery was achieved. A DD cell was introduced to overcome the scaling of the CEM; at the same Load Ratio,  $L_N=1$ , and at  $10 \text{ A m}^{-2}$ , the TAN recovery was 82% when using synthetic influent. This experiment was carried out over 5 days. When using digested black water, the TAN recovery was 72.5% over 36 h. Without DD, 1.2 g ammonium were supplied, 0.9 g were recovered in the acid, and 0.3 g were found in the effluent. With DD, 2.8 g ammonium were supplied, 2.1 g were recovered in the acid, and 0.7 g were found in the effluent. The TAN recovery efficiency was affected by operating with real wastewater and by operating the ED combined with DD. Nevertheless, as the system operated during a three times longer period with Donnan, although the TAN recovery was reduced, more influent was treated and consequently more nitrogen was recovered.

Furthermore, the energy consumption was nearly constant, independent of Donnan dialysis and the influent composition. Operating the system consumed around  $8 \text{ kWh kg}_N^{-1}$  (SI, Figure A.2). The energy consumption can be explained when we look at the potential losses (SI, Figure A.2). Ionic losses occur due to the transport of ions and are thus, dependent on the conductivity of the solution. The conductivity of the

digested black water was  $6.5 \text{ mS cm}^{-1}$  on average resulting in higher potential losses compared to influents such as urine (around  $29 \text{ mS cm}^{-1}$ ) or reject water (around  $12 \text{ mS cm}^{-1}$ ), as previously shown. (Rodrigues et al., 2020a, 2020b; Sleutels et al., 2017, 2013) The fluctuation of MEA overpotential was not expected. The MEA overpotential is the difference between the measured anode potential and the theoretical anode potential. If the contact between  $\text{H}_2$  gas and gas diffusion electrode is not efficient, then the MEA overpotential can increase. (Post et al., 2009) Also, scaling and biofouling of the cation exchange membrane in the MEA can also cause an increase of the MEA overpotential. (Choi et al., 2011; Ping et al., 2013) However, we observed that the MEA overpotential was independent of the influent supplied to the system (SI, Figure A.2). Thus, we suspect that the MEA could have suffered some unexpected damage (not further identified) leading to a fluctuation in the potential loss.

### 3.2. The performance was enhanced and the operation window was expanded by operating at higher Load Ratio

We evaluated the ES performance with DD cell regarding TAN recovery efficiency and energy consumption for different nitrogen loading at constant current (Load Ratio) (Fig. 3).

Fig. 3 shows that the overall TAN recovery and energy consumption of the ES combined with Donnan dialysis increased with Load Ratio. This phenomenon is in accordance with the Load Ratio model previously established for electrochemical systems for TAN recovery (Rodríguez Arredondo et al., 2017). At Load ratio 1.3, TAN recovery of 83% was achieved, whereas for Load Ratio 1.5, the TAN recovery was 85%. As no significant improvement was observed for Load Ratio 1.5, no higher Load Ratio were tested. The presented energy consumption is the



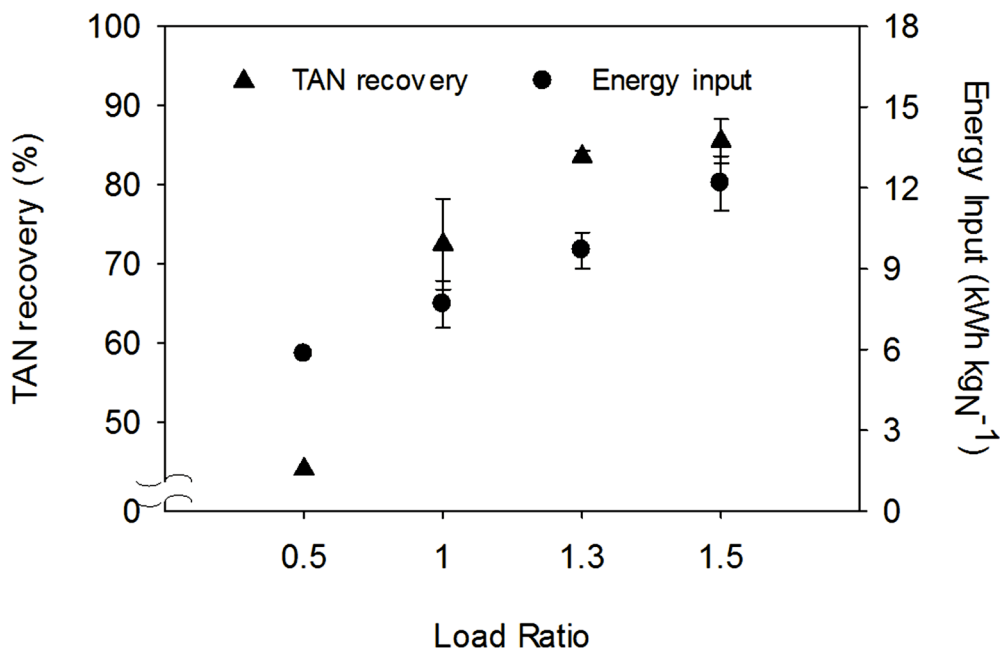


**Fig. 3.** TAN Recovery and Energy Input of the ES treating digested black water with Donnan dialysis at different Load Ratio. TAN recovery and energy consumption increased with Load Ratio. The combined system achieved up to 85% TAN recovery.

average for each experiment operated with ES including DD cell using filtered digested black water at Load Ratios 0.5, 1, 1.3 and 1.5. The average does not consider the last day of each experiment as the voltage ramped up and consequently the operation was interrupted (SI, Figure A.3). During stable operation the electrodialysis with Donnan dialysis treated in total 2.4 L for Load Ratio 0.5, 3.5 L for Load ratio 1, 5.2 L for Load Ratio 1.3, and 4.8 L for Load Ratio 1.5. The combined system consumed between 5.8 kWh kgN<sup>-1</sup> for Load Ratio 0.5 and 12.2 kWh kgN<sup>-1</sup> for Load Ratio 1.5. The ES operated without the DD cell consumed around 7.5 kWh kgN<sup>-1</sup> during the 12 h of operation at Load

Ratio one.

### 3.3. Donnan dialysis enables ammonia recovery from a complex wastewater including calcium ions, by regulating the pH at 9.7

Fig. 4 represents the average charge species transported over the CEM on the electrodialysis cell (A) and over the CEM in the DD cell (B) for different Load Ratio and a current density of 10 A m<sup>-2</sup>.

Fig. 4 shows the average ion transport before the experiments were interrupted due to the extreme cell voltage increase. The average

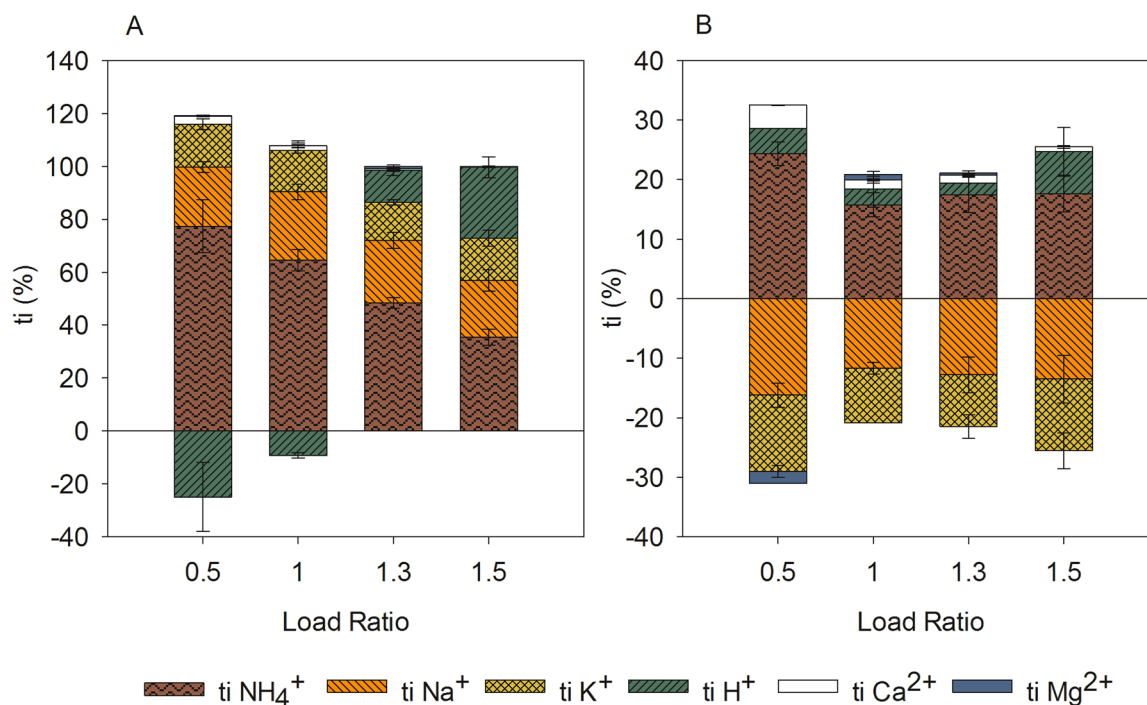


**Fig. 4.** A). Transported charge over the CEM in the electrodialysis cell system. B) Exchanged charge over the CEM in the DD cell. The measured transported species were NH<sub>4</sub><sup>+</sup>, Na<sup>+</sup>, K<sup>+</sup>, Ca<sup>2+</sup>, Mg<sup>2+</sup>, and H<sup>+</sup>.

transport for each ion was calculated up to the point that scaling was detected. Scaling affects the ion flux as previously demonstrated by Asraf-Snir et al., 2018 and can be detected by the voltage increase (Asraf-Snir et al., 2018). Overall, ammonium is the dominant charge carrier (highest  $t_i$ ), followed by sodium and potassium, shown in Fig. 4A. The ionic composition of the influent and the Load Ratio affect the transport of charged species over the CEM in the electro dialysis cell. The relative ammonium transport decreased with increasing Load Ratio, while the proton transport increased accordingly. Sodium ( $0.23 \pm 0.02$ ) and potassium ( $0.16 \pm 0.01$ ) transport remain constant, probably due ion exchange during the Donnan dialysis pre-treatment.

Once a gradient is formed between feed and concentrate, potassium ( $K^+$ ) and sodium ( $Na^+$ ) are exchanged with ammonium ( $NH_4^+$ ) and protons ( $H^+$ ) in the DD cell (Fig. 4B). For Load Ratio higher than one, calcium ( $Ca^{2+}$ ) and magnesium ( $Mg^{2+}$ ) are both transported to the concentrate compartment through the Donnan and electro dialysis CEMs. Magnesium was only returned to the feed at Load Ratio 0.5. Moreover, calcium and magnesium only represented less than 5% of the charge exchange. The desired transport of calcium ions to the feed did not occur.

In this study, up to 4 mmol (150 mg) of calcium was removed from the supplied influent by DD+ED. Calcite ( $CaCO_3$ ) precipitation occurs even at very low concentrations and pH just slightly above neutral conditions (Hasson et al., 2010). This precipitation can occur simultaneously on the surface and at the pores of the membrane. With a continuous electric field transporting cations through the CEM, a high enough concentration at the membrane solution interface induced precipitation (Ayala-Bribiesca et al., 2006; Belashova et al., 2017), causing the obstruction of the membrane pores and possibly membrane dehydration. In our system magnesium was also removed to a certain extent, and while the analyzed membranes did not show any magnesium salt precipitates, its contribution on facilitating calcium precipitation was previously demonstrated.

The considerable increase of membrane resistance (SI, Figure A.3), which is related to the increase of membrane potential, is the result of scaling formation at the cation exchange membrane. Here, CEMs become more resistant to ion transport, and as a result water splitting at the surface of the membrane is enhanced (Andreeva et al., 2018; Asraf-Snir et al., 2018). The high membrane potential coincides with an

increase in the pH of the concentrate.

Fig. 5 is the average pH measured over each 12 h in feed and concentrate solutions for different Load Ratios.

Fig. 5 also shows that the average pH of the concentrate is approximately 10 during the first 12 h. For Load Ratio 1.3 and 1.5, the pH of the concentrate was stable for almost three to four days at pH 9.7 with Donnan dialysis; conversely, when operating without Donnan dialysis, the pH rapidly reached 11.6. A comparison of Fig. 5 with Figure A.3 (SI) reveals that the membrane loss increases sharply when the concentrate pH reached 12. Donnan dialysis thus acts, to a certain extent, as a pH regulator, an effect that is enhanced with increased Load Ratio. The transport of protons for high Load Ratio in the electro dialysis cell, combined with the protons exchanged in DD cell, decreased the pH of the concentrate (Fig. 5). Although the pH was lower, the concentration of calcium on the concentrate side increased with time reaching a saturation point. Earlier experiments have shown that calcium carbonate precipitates at a pH as low as 8.6 (Koutsoukos and Kontoyannis, 1984; Söhnel and Mullin, 1982). After scaling precipitation, the CEM was restored with an acid cleaning. In the experiments presented here, Donnan dialysis extended the operation period and therefore reduced the chemical need as the frequency of cleaning is reduced. Although Donnan dialysis extended the operation period and therefore reduced the chemical need, it can still be combined with a in situ cleaning to guarantee the long term operation of the ES operation.

Thompson-Brewster et al., 2017 predicted the major scaling site occurring in electrochemical recovery of ammonium to be in the double layer on the concentrate side of the CEM. The model described how two different pre-treatments can reduce the occurrence of scaling (such as struvite) (Thompson Brewster et al., 2017). In our study, the predominant anion responsible for scaling was carbonate unlike previous studies that observed phosphate or sulfate precipitation (Asraf-Snir et al., 2018; Thompson Brewster et al., 2017). As the CEM blocks anions, we believe  $CO_2$  formed in acidic conditions is transported by diffusion through the CEM and forms carbonate under alkaline conditions in the concentrate solution (Legrand et al., 2020; Nikonenko et al., 2003; Paz-Garcia et al., 2014).

As previous work has shown, the membrane structure and influent composition must be considered when designing an electro dialysis cell for nutrient recovery (Andreeva et al., 2017; Asraf-Snir et al., 2018;

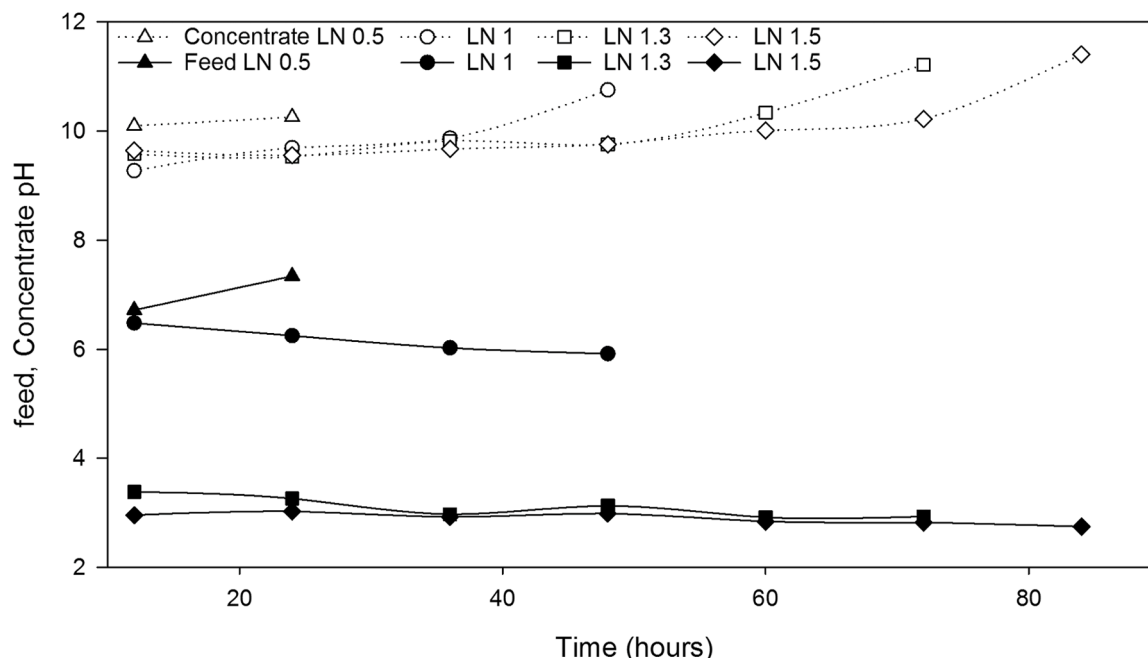


Fig. 5. Average pH measured in the feed (solid fill) and concentrate (empty fill) solutions over time for different Load Ratio (LN).

Belashova et al., 2017). Bivalent ions are present in several (source separated) wastewater streams such as black water and urine (Shi et al., 2018; Thompson Brewster et al., 2017). Pre-treatments that simultaneously minimize the application of chemicals, maintain the overall energy demand, and limit additional capital investments should be further investigated to prevent scaling and consequently improve the system performance (Asraf-Snir et al., 2018; Zabolotsky et al., 1997). By combining electro dialysis and Donnan dialysis, we extended the operation of an electrochemical system supplied with a complex wastewater from 12 hour to 36 h at the same nitrogen load vs applied current. The period of operation was further extended from 36 h up to 84 h by increasing the Load Ratio from 1 to 1.5. Moreover, the combined system was able to effectively remove the ammonium present in the influent (to less than 100 mg L<sup>-1</sup> in the effluent).

Future research should include the performance of the system at higher current densities and the use of other more concentrated streams such as manure.

#### 4. Conclusion

Donnan dialysis delayed the scaling effect on cation exchange membranes, allowing the operation of an electro dialysis system for a longer period without interruption for cleaning. At the same Load ratio and current density, the combined system operated for 24 h more than a stand-alone electrochemical system, before the cell voltage increased significantly. Here, Donnan dialysis acted as a pH regulator of the concentrate solution and consequently delayed calcite (CaCO<sub>3</sub>) precipitation. By increasing the current compared to the TAN loading (Load ratio), the operation window was further extended up to 72 h and consequently increasing the treatment capacity, while maintaining a high TAN recovery of 83% and consuming 9.7 kWh gN<sup>-1</sup>.

#### Associated content

Supporting information are available free of charge.

#### Research data

The research data underlying this work is available at <https://doi.org/10.4121/14039495>.

#### Declaration of Competing Interest

None.

#### Acknowledgments

This work was performed in the cooperation framework of Wetsus, European centre of Excellence for Sustainable Water Technology ([www.wetsus.eu](http://www.wetsus.eu)). Wetsus is co-funded by the Dutch Ministry of Economic Affairs and Ministry of Infrastructure and Environment, the European Union Regional Development Fund, the Province of Fryslân, and the Northern Netherlands Provinces. This work was also supported by the LIFE-NEWBIES project. The LIFE-NEWBIES project (LIFE17 ENV/NL/00408) has received funding from the LIFE Programme of the European Union. The authors like to thank the participants of the research theme “Resource Recovery” for the fruitful discussions and their financial support. The authors would also like to thank Chris Schott (Wetsus & Wageningen University) for collecting the black water, operating the UASB reactor and supplying the influent (digested black water) for characterization of our system.

#### Supplementary materials

Supplementary material associated with this article can be found, in the online version, at doi:[10.1016/j.watres.2021.117260](https://doi.org/10.1016/j.watres.2021.117260).

#### References

- Ahn, Y.H., 2006. Sustainable nitrogen elimination biotechnologies: a review. *Process Biochem.* 41, 1709–1721. <https://doi.org/10.1016/j.procbio.2006.03.033>.
- Andreeva, M.A., Gil, V.V., Pismenskaya, N.D., Dammak, L., Kononenko, N.A., Larchet, C., Grande, D., Nikonenko, V.V., 2018. Mitigation of membrane scaling in electro dialysis by electroconvection enhancement, pH adjustment and pulsed electric field application. *J. Memb. Sci.* 549, 129–140. <https://doi.org/10.1016/j.memsci.2017.12.005>.
- Andreeva, M.A., Gil, V.V., Pismenskaya, N.D., Nikonenko, V.V., Dammak, L., Larchet, C., Grande, D., Kononenko, N.A., 2017. Effect of homogenization and hydrophobization of a cation-exchange membrane surface on its scaling in the presence of calcium and magnesium chlorides during electro dialysis. *J. Memb. Sci.* 540, 183–191. <https://doi.org/10.1016/j.memsci.2017.06.030>.
- Asraf-Snir, M., Gilron, J., Oren, Y., 2018. Scaling of cation exchange membranes by gypsum during Donnan exchange and electro dialysis. *Journal of Membrane Science*. Elsevier B.V. <https://doi.org/10.1016/j.memsci.2018.08.009>.
- Ayala-Bribiesca, E., Pourcelly, G., Bazinet, L., 2006. Nature identification and morphology characterization of cation-exchange membrane fouling during conventional electro dialysis. *J. Colloid Interface Sci.* 300, 663–672. <https://doi.org/10.1016/j.jcis.2006.04.035>.
- Belashova, E., Mikhaylin, S., Pismenskaya, N., Nikonenko, V., Bazinet, L., 2017. Impact of cation-exchange membrane scaling nature on the electrochemical characteristics of membrane system. *Sep. Purif. Technol.* 189, 441–448. <https://doi.org/10.1016/j.seppur.2017.08.045>.
- Campione, A., Gurreri, L., Ciofalo, M., Micale, G., Tamburini, A., Cipollina, A., 2018. Electro dialysis for water desalination: a critical assessment of recent developments on process fundamentals, models and applications. *Desalination* 434, 121–160. <https://doi.org/10.1016/j.desal.2017.12.044>.
- Casademont, C., Farias, M.A., Pourcelly, G., Bazinet, L., 2008. Impact of electro dialytic parameters on cation migration kinetics and fouling nature of ion-exchange membranes during treatment of solutions with different magnesium/calcium ratios. *J. Memb. Sci.* 325, 570–579. <https://doi.org/10.1016/j.memsci.2008.08.023>.
- Casademont, C., Pourcelly, G., Bazinet, L., 2007. Effect of magnesium/calcium ratio in solutions subjected to electro dialysis: characterization of cation-exchange membrane fouling. *J. Colloid Interface Sci.* 315, 544–554. <https://doi.org/10.1016/j.jcis.2007.06.056>.
- Chen, C., Dong, T., Han, M., Yao, J., Han, L., 2020. Ammonium recovery from wastewater by Donnan Dialysis: a feasibility study. *J. Clean. Prod.* 265, 121838. <https://doi.org/10.1016/j.jclepro.2020.121838>.
- Choi, M.J., Chae, K.J., Ajayi, F.F., Kim, K.Y., Yu, H.W., Kim, C., Kim, I.S., 2011. Effects of biofouling on ion transport through cation exchange membranes and microbial fuel cell performance. *Bioreour. Technol.* 102, 298–303. <https://doi.org/10.1016/j.biortech.2010.06.129>.
- Cordell, D., Drangert, J.O., White, S., 2009. The story of phosphorus: global food security and food for thought. *Glob. Environ. Chang.* 19, 292–305. <https://doi.org/10.1016/j.gloenvcha.2008.10.009>.
- Cordell, D., Rosemarin, A., Schröder, J.J., Smit, A.L., 2011. Towards global phosphorus security: a systems framework for phosphorus recovery and reuse options. *Chemosphere* 84, 747–758. <https://doi.org/10.1016/j.chemosphere.2011.02.032>.
- Cox, J.A., Dinunzio, J.E., 1977. Donnan Dialysis Enrichment of Cations. *Anal. Chem.* 49, 1272–1275. <https://doi.org/10.1021/ac50016a056>.
- Cunha, J.R., Schott, C., van der Weijden, R.D., Leal, L.H., Zeeman, G., Buisman, C.J.N., 2019. Recovery of calcium phosphate granules from black water using a hybrid upflow anaerobic sludge bed and gas-lift reactor. *Environ. Res.* 178, 108671. <https://doi.org/10.1016/j.envres.2019.108671>.
- Cunha, J.R., Schott, C., van der Weijden, R.D., Leal, L.H., Zeeman, G., Buisman, C.J.N., 2018. Calcium addition to increase the production of phosphate granules in anaerobic treatment of black water. *Water Res.* 130, 333–342. <https://doi.org/10.1016/j.watres.2017.12.012>.
- de Graaff, M.S., Temmink, H., Zeeman, G., Buisman, C.J.N., 2010. Anaerobic treatment of concentrated black water in a UASB reactor at a short HRT. *Water (Basel)* 2, 101–119. <https://doi.org/10.3390/w2010101>.
- Egle, L., Rechberger, H., Krampe, J., Zessner, M., 2016. Phosphorus recovery from municipal wastewater: an integrated comparative technological, environmental and economic assessment of P recovery technologies. *Sci. Total Environ.* <https://doi.org/10.1016/j.scitotenv.2016.07.019>.
- Galloway, J.N., Townsend, A.R., Erismann, J.W., Bekunda, M., Cai, Z., Freney, J.R., Martinelli, L.A., Seitzinger, S.P., Sutton, M.A., 2008. Transformation of the Nitrogen Cycle. *Science* (80-) 320, 889–892. <https://doi.org/10.1126/science.1136674>.
- Gao, M., Zhang, L., Florentino, A.P., Liu, Y., 2019. Performance of anaerobic treatment of blackwater collected from different toilet flushing systems: can we achieve both energy recovery and water conservation? *J. Hazard. Mater.* 365, 44–52. <https://doi.org/10.1016/j.jhazmat.2018.10.055>.
- Giddey, S., Badwal, S.P.S., Kulkarni, A., 2013. Review of electrochemical ammonia production technologies and materials. *Int. J. Hydrogen Energy.* <https://doi.org/10.1016/j.ijhydene.2013.09.054>.
- Hasson, D., Sidorenko, G., Semiat, R., 2010. Calcium carbonate hardness removal by a novel electrochemical seeds system. *Desalination* 263, 285–289. <https://doi.org/10.1016/j.desal.2010.06.036>.
- Koutsoukos, P.G., Kontoyannis, C.G., 1984. Precipitation of calcium carbonate in aqueous solutions. *J. Chem. Soc. Faraday Trans. 1 Phys. Chem. Condens. Phases* 80, 1181–1192. <https://doi.org/10.1039/F19848001181>.
- Kuntke, P., Rodrigues, M., Sleutels, T., Saakes, M., Hamelers, H.V.M., Buisman, C.J.N., 2018a. Energy-efficient ammonia recovery in an up-scaled hydrogen gas recycling

- electrochemical system. *ACS Sustain. Chem. Eng.* acssuschemeng.8b00457. <https://doi.org/10.1021/acssuschemeng.8b00457>.
- Kuntke, P., Rodríguez Arredondo, M., Widyakristi, L., ter Heijne, A., Sleutels, T.H.J.A., Hamelers, H.V.M., Buisman, C.J.N., 2017. Hydrogen gas recycling for energy efficient ammonia recovery in electrochemical systems. *Environ. Sci. Technol.* 51, 3110–3116. <https://doi.org/10.1021/acs.est.6b06097>.
- Kuntke, P., Sleutels, T.H.J.A., Rodríguez Arredondo, M., Georg, S., Barbosa, S.G., ter Heijne, A., Hamelers, H.V.M., Buisman, C.J.N., 2018b. (Bio)electrochemical ammonia recovery: progress and perspectives. *Appl. Microbiol. Biotechnol.* 102, 3865–3878. <https://doi.org/10.1007/s00253-018-8888-6>.
- Larsen, T.A., Udert, K.M., Lienert, J., 2015. Source Separation and Decentralization for Wastewater Management, Source Separation and Decentralization for Wastewater Management. <https://doi.org/10.2166/9781780401072>.
- Ledezma, P., Kuntke, P., Buisman, C.J.N., Keller, J., Freguia, S., 2015. Source-separated urine opens golden opportunities for microbial electrochemical technologies. *Trends Biotechnol.* <https://doi.org/10.1016/j.tibtech.2015.01.007>.
- Legrand, L., Shu, Q., Tedesco, M., Dykstra, J.E., Hamelers, H.V.M., 2020. Role of ion exchange membranes and capacitive electrodes in membrane capacitive deionization (MCDI) for CO<sub>2</sub> capture. *J. Colloid Interface Sci.* 564, 478–490. <https://doi.org/10.1016/j.jcis.2019.12.039>.
- Lei, X., Sugiura, N., Feng, C., Maekawa, T., 2007. Pretreatment of anaerobic digestion effluent with ammonia stripping and biogas purification. *J. Hazard. Mater.* 145, 391–397. <https://doi.org/10.1016/j.jhazmat.2006.11.027>.
- Lei, Y., Du, M., Kuntke, P., Saakes, M., Van Der Weijden, R., Buisman, C.J.N., 2019. Energy efficient phosphorus recovery by microbial electrolysis cell induced calcium phosphate precipitation. *ACS Sustain. Chem. Eng.* 7, 8860–8867. <https://doi.org/10.1021/acssuschemeng.9b00867>.
- Luther, A.K., Desloover, J., Fennell, D.E., Rabaey, K., 2015. Electrochemically driven extraction and recovery of ammonia from human urine. *Water Res.* 87, 367–377. <https://doi.org/10.1016/j.watres.2015.09.041>.
- Maurer, M., Schwegler, P., Larsen, T.A., 2003. Nutrients in urine: energetic aspects of removal and recovery. *Water Sci. Technol.* 48, 37–46. <https://doi.org/10.1017/S000748530002229X>.
- Moges, M.E., Todt, D., Heistad, A., 2018. Treatment of source-separated blackwater: a decentralized strategy for nutrient recovery towards a circular economy. *Water (Switzerland)* 10. <https://doi.org/10.3390/w10040463>.
- Nikonenko, V., Lebedev, K., Manzanarez, J.A., Pourcelly, G., 2003. Modelling the transport of carbonic acid anions through anion-exchange membranes. *Electrochim. Acta* 48, 3639–3650. [https://doi.org/10.1016/S0013-4686\(03\)00485-7](https://doi.org/10.1016/S0013-4686(03)00485-7).
- Pan, Y., Zhu, T., He, Z., 2020. Minimizing effects of chloride and calcium towards enhanced nutrient recovery from sidestream centrate in a decoupled electro dialysis driven by solar energy. *J. Clean. Prod.* 263, 121419. <https://doi.org/10.1016/j.jclepro.2020.121419>.
- Paz-Garcia, J.M., Schaetzle, O., Biesheuvel, P.M., Hamelers, H.V.M., 2014. Energy from CO<sub>2</sub> using capacitive electrodes - Theoretical outline and calculation of open circuit voltage. *J. Colloid Interface Sci.* 418, 200–207. <https://doi.org/10.1016/j.jcis.2013.11.081>.
- Ping, Q., Cohen, B., Dosoretz, C., He, Z., 2013. Long-term investigation of fouling of cation and anion exchange membranes in microbial desalination cells. *Desalination* 325, 48–55. <https://doi.org/10.1016/j.desal.2013.06.025>.
- Post, J.W., Hamelers, H.V.M., Buisman, C.J.N., 2009. Influence of multivalent ions on power production from mixing salt and fresh water with a reverse electro dialysis system. *J. Memb. Sci.* 330, 65–72. <https://doi.org/10.1016/j.memsci.2008.12.042>.
- Rijnaarts, T., Shenkute, N.T., Wood, J.A., De Vos, W.M., Nijmeijer, K., 2018. Divalent cation removal by donnan dialysis for improved reverse electro dialysis. *ACS Sustain. Chem. Eng.* 6, 7035–7041. <https://doi.org/10.1021/acssuschemeng.8b00879>.
- Rodrigues, M., De Mattos, T.T., Sleutels, T., Heijne, Ter, A., Hamelers, H.V.M., Buisman, C.J.N., Kuntke, 2020a. Minimal bipolar membrane cell configuration for scaling up ammonium recovery. *ACS Sustain. Chem. Eng.* 8, 17359–17367. <https://doi.org/10.1021/acssuschemeng.0c05043>.
- Rodrigues, M., Sleutels, T., Kuntke, P., Hoekstra, D., ter Heijne, A., Buisman, C.J.N., Hamelers, H.V.M., 2020b. Exploiting Donnan Dialysis to enhance ammonia recovery in an electrochemical system. *Chem. Eng. J.* 395, 125143. <https://doi.org/10.1016/j.cej.2020.125143>.
- Rodríguez Arredondo, M., Kuntke, P., Jeremiasse, A.W., Sleutels, T.H.J.A., Buisman, C.J.N., ter Heijne, A., 2015. Bioelectrochemical systems for nitrogen removal and recovery from wastewater. *Environ. Sci. Water Res. Technol.* 1, 22–33. <https://doi.org/10.1039/C4EW00066H>.
- Rodríguez Arredondo, M., Kuntke, P., ter Heijne, A., Hamelers, H.V.M., Buisman, C.J.N., 2017. Load ratio determines the ammonia recovery and energy input of an electrochemical system. *Water Res.* 111, 330–337. <https://doi.org/10.1016/j.watres.2016.12.051>.
- Shaposhnik, V.A., Zubets, N.N., Strygina, I.P., Mill, B.E., 2002. High demineralization of drinking water by electro dialysis without scaling on the membranes. *Desalination* 145, 329–332. [https://doi.org/10.1016/S0011-9164\(02\)00431-9](https://doi.org/10.1016/S0011-9164(02)00431-9).
- Shi, L., Hu, Y., Xie, S., Wu, G., Hu, Z., Zhan, X., 2018. Recovery of nutrients and volatile fatty acids from pig manure hydrolysate using two-stage bipolar membrane electro dialysis. *Chem. Eng. J.* 334, 134–142. <https://doi.org/10.1016/j.cej.2017.10.010>.
- Shipman, M.A., Symes, M.D., 2017. Recent progress towards the electrosynthesis of ammonia from sustainable resources. *Catal. Today* 286, 57–68. <https://doi.org/10.1016/j.cattod.2016.05.008>.
- Sleutels, T.H.J.A., Heijne, A., Ter, Buisman, C.J.N., Hamelers, H.V.M., 2013. Steady-state performance and chemical efficiency of Microbial Electrolysis Cells. *Int. J. Hydrogen Energy* 38, 7201–7208. <https://doi.org/10.1016/j.ijhydene.2013.04.067>.
- Sleutels, T.H.J.A., ter Heijne, A., Kuntke, P., Buisman, C.J.N., Hamelers, H.V.M., 2017. Membrane selectivity determines energetic losses for ion transport in bioelectrochemical systems. *ChemistrySelect* 2, 3462–3470. <https://doi.org/10.1002/slct.201700064>.
- Söhnle, O., Mullin, J.W., 1982. Precipitation of calcium carbonate. *J. Cryst. Growth* 60, 239–250. [https://doi.org/10.1016/0022-0248\(82\)90095-1](https://doi.org/10.1016/0022-0248(82)90095-1).
- Tarpeh, W.A., Barazesh, J.M., Cath, T.Y., Nelson, K.L., 2018. Electrochemical stripping to recover nitrogen from source-separated urine. *Environ. Sci. Technol.* 52, 1453–1460. <https://doi.org/10.1021/acs.est.7b05488>.
- Theregowda, R.B., González-Mejía, A.M., Ma, X., Garland, J., 2019. Nutrient recovery from municipal wastewater for sustainable food production systems: an alternative to traditional fertilizers. *Environ. Eng. Sci.* 36, 833–842. <https://doi.org/10.1089/ees.2019.0053>.
- Thompson Brewster, E., Ward, A.J., Mehta, C.M., Radjenovic, J., Batstone, D.J., 2017. Predicting scale formation during electro dialytic nutrient recovery. *Water Res.* 110, 202–210. <https://doi.org/10.1016/j.watres.2016.11.063>.
- Tran, A.T.K., Jullok, N., Meesschaert, B., Pinoy, L., Van der Bruggen, B., 2013. Pellet reactor pretreatment: a feasible method to reduce scaling in bipolar membrane electro dialysis. *J. Colloid Interface Sci.* 401, 107–115. <https://doi.org/10.1016/j.jcis.2013.03.036>.
- Vlaeminck, S.E., Terada, A., Smets, B.F., Van Der Linden, D., Boon, N., Verstraete, W., Carballa, M., 2009. Nitrogen removal from digested black water by one-stage partial nitrification and anammox. *Environ. Sci. Technol.* 43, 5035–5041. <https://doi.org/10.1021/es803284y>.
- Wasielewski, S., Morandi, C.G., Minke, R., Steinmetz, H., 2016. Ammonium Recovery By Ion Exchange from Effluents of Anaerobic Blackwater Co-Digestion and Struvite Precipitation Reactors.
- Wilfert, P., Kumar, P.S., Korving, L., Witkamp, G.J., Van Loosdrecht, M.C.M., 2015. The Relevance of Phosphorus and Iron Chemistry to the Recovery of Phosphorus from Wastewater: A Review. *Environmental Science and Technology*. <https://doi.org/10.1021/acs.est.5b00150>.
- Yang, Y., Gao, X., Fan, A., Fu, L., Gao, C., 2014. An innovative beneficial reuse of seawater concentrate using bipolar membrane electro dialysis. *J. Memb. Sci.* 449, 119–126. <https://doi.org/10.1016/j.memsci.2013.07.066>.
- Zabolotsky, V.I., Nikonenko, V.V., Pismenskaya, N.D., Istoshin, A.G., 1997. Electro dialysis technology for deep demineralization of surface and ground water. *Desalination* 108, 179–181. [https://doi.org/10.1016/S0011-9164\(97\)00025-8](https://doi.org/10.1016/S0011-9164(97)00025-8).
- Zamora, P., Georgieva, T., Salcedo, I., Elzinga, N., Kuntke, P., Buisman, C.J.N., 2017. Long-term operation of a pilot-scale reactor for phosphorus recovery as struvite from source-separated urine. *J. Chem. Technol. Biotechnol.* 92, 1035–1045. <https://doi.org/10.1002/jctb.5079>.
- Zeeman, G., Kujawa-Roeleveld, K., 2011. Resource recovery from source separated domestic waste(water) streams; full scale results. *Water Sci. Technol.* 64, 1987–1992. <https://doi.org/10.2166/wst.2011.562>.